

Low-alkali metal content in β -vanadium mixed bronzes: The crystal structures of β - $K_x(V,Mo)_6O_{15}$ ($x = 0.23$ and 0.32) by single-crystal X-ray diffraction

Michele Zema^{a,*}, Paolo Ghigna^b, Serena C. Tarantino^a

^aDipartimento di Scienze della Terra, Università di Pavia, via Ferrata 1, 27100 Pavia, Italy

^bDipartimento di Chimica Fisica “M. Rolla”, Università di Pavia, v.le Taramelli 16, 27100 Pavia, Italy

Received 5 July 2006; received in revised form 13 November 2006; accepted 15 November 2006

Available online 18 November 2006

Abstract

The vanadium–molybdenum mixed oxide bronzes of composition $K_{0.23}(V_{5.35}Mo_{0.65})O_{15}$ and $K_{0.32}(V_{5.48}Mo_{0.52})O_{15}$ have a monoclinic structure with s.g. $C2/m$, $Z = 2$, and unit-cell dimensions $a = 15.436(2)$, $b = 3.6527(5)$, $c = 10.150(1)$ Å, $\beta = 108.604(3)^\circ$ and $a = 15.452(2)$, $b = 3.6502(5)$, $c = 10.142(1)$ Å, $\beta = 109.168(3)^\circ$, respectively, as determined by single-crystal X-ray diffraction. These compounds show the β - $Na_xV_6O_{15}$ tunnel structure, which is isostructural with bannermanite, natural sodium–potassium vanadate. Structure refinements from diffracted intensities collected in the 2 – $38^\circ 2\theta$ range converged to final $R = 5.58\%$ and 7.48% for the two crystals, respectively. The V atoms are distributed on three different crystallographic sites. Partial substitution of V with Mo occurs in only one of these positions. Oxygen atoms involved in vanadyl groups point toward the tunnels. The K ions in the tunnels are coordinated by seven oxygen atoms. The alkali metal content in these crystals is much lower than the solubility limit found for the analogous Na containing compound.

© 2006 Elsevier Inc. All rights reserved.

Keywords: Molybdenum–vanadium bronzes; Tunnel structure; Bannermanite; X-ray diffraction; Crystal structure

1. Introduction

Vanadium oxide bronzes of general formula $M_xV_2O_5$, with typical non-stoichiometry in the intercalated M metal ion and mixed valency of the vanadium ions (V^{4+} and V^{5+}), unlike the bronzes of other transition metals, form a wide variety of structures and represent an exceptionally flexible family of phases, containing examples of both layered (α -phase) and tunnel (β -phase) framework structures ([1], and references therein). This variety is due to the relatively small size and range in ionic-covalent nature of the vanadium ion as compared to other oxide bronze forming transition metals. Whereas the larger transition metal ions form a regular covalent network of octahedra, the vanadium octahedra are often distorted, even to the point of forming five-coordinated square-based pyramids.

This distortion results in complex vanadium bronze structure types and imparts a strong anisotropy to some of their physical properties.

The flexibility of these structures allows the intercalation of a wide range of ions (Li^+ , Na^+ , K^+ , Ag^+ , NH_4^{4+} , Mg^{2+} , Ca^{2+} , Fe^{2+} , Cu^+ , Cu^{2+} , Sr^{2+} , Pb^{2+} , etc.) [2–8]. Among these, sodium vanadium oxide bronze family $Na_xV_x^{4+}V_{6-x}^{5+}O_{15}$ (to which $K_xV_6O_{15}$ is isostructural) [9] has been widely studied since the pioneering works by Flood and Sorum [10] and Wadsley [11], the latter providing also the structural explanation for the non-stoichiometric nature of the compound. A number of polymorphs are known for x ranging between 0 and 6 for $Na_xV_6O_{15}$ [2,12–14]. For very low Na contents ($0 \leq x \leq 0.06$), the layered orthorhombic α - $Na_xV_6O_{15}$, isostructural with mineral shcherbinaite V_2O_5 , is stable. With increasing Na concentration, the monoclinic β -phase, showing the bannermanite-type tunnel structure, is formed with compositional limits of $0.66 \leq x \leq 1.0$ [15]. The β - $Na_xV_6O_{15}$ phase has

*Corresponding author. Fax: +39 0382 985890.

E-mail address: zema@crystal.unipv.it (M. Zema).

recently gained increased interest because of the discovery of superconductivity under high pressure [16] and for its application as rechargeable electrodes [17] and ion-selective devices [18].

Natural occurring bannermanite $(\text{Na}, \text{K})_x \text{V}_x^{4+} \text{V}_{6-x}^{5+} \text{O}_{15}$ ($0.54 \leq x \leq 0.90$) has been discovered in association with shcherbinaite, stoiberite and ziesite in the fumaroles in the summit crater of Izalco volcano, El Salvador, Central America [19] and has been thoroughly characterized by Hughes and Finger [20].

In the search of new materials containing ions of large ionic radius and tunnel structures, vanadium–molybdenum substitution has been proposed [21]. Recently, a new vanadium–molybdenum mixed bronze family with stoichiometry $A_x(\text{Mo}, \text{V})_8 \text{O}_{21}$ ($A = \text{K}^+, \text{Rb}^+, \text{Cs}^+$) has been reported [22]. A detailed analysis of the compositional diagram of the series $\beta\text{-}M_x \text{V}_{6-y} \text{T}_y \text{O}_{15}$ ($M = \text{Na}, \text{Li}; T = \text{Mo}, \text{W}$) has been given by Darriet et al. [23,24], who also characterized the crystal structure of the $\beta\text{-Na}_x \text{V}_{6-y} \text{Mo}_y \text{O}_{15}$ phase with different V/Mo ratios.

In this work, we present structural investigations of two samples, $\text{K}_{0.23}(\text{V}_{5.35} \text{Mo}_{0.65}) \text{O}_{15}$ and $\text{K}_{0.32}(\text{V}_{5.48} \text{Mo}_{0.52}) \text{O}_{15}$,

which crystallize with the bannermanite-type $\beta\text{-Na}_x \text{V}_6 \text{O}_{15}$ structure. This allows to extend the knowledge on this compounds family by characterizing β -vanadium mixed bronzes with potassium as intercalated ion. The studied compounds show a K content fairly lower than the known compositional limit of the monovalent cation in the Na β -series.

2. Experimental

2.1. Synthesis

Acicular single crystals of $\text{K}_x(\text{V}_{6-y} \text{Mo}_y) \text{O}_{15}$ were obtained as by-products of a synthesis of VOMoO_4 single crystals by the chemical transport method. In particular, an equimolar mixture of VO_2 (Aldrich, 99%) and MoO_3 (Aldrich, 99.5%) was suspended in CHCl_3 and stirred overnight, until the complete evaporation of CHCl_3 . A total of 10% in weight of TeCl_4 (Aldrich, 95%) was then added and mixed with a mortar and pestle. The mixture was then pressed to pellets and sealed under vacuum in a quartz vial. A platinum boat was used to avoid the contact

Table 1
Crystal and refinement data

Chemical formula	$\text{K}_{0.23}(\text{V}_{5.35} \text{Mo}_{0.65}) \text{O}_{15}$	$\text{K}_{0.32}(\text{V}_{5.48} \text{Mo}_{0.52}) \text{O}_{15}$
F_w	583.88	581.56
Crystal shape	Needle	Needle
Crystal size (mm)	$0.48 \times 0.03 \times 0.03$	$0.12 \times 0.01 \times 0.01$
Crystal system	Monoclinic	Monoclinic
Space group	$C2/m$	$C2/m$
a (Å)	15.4358(20)	15.4520(11)
b (Å)	3.6527(5)	3.6502(3)
c (Å)	10.1499(13)	10.1420(8)
β (°)	108.604(3)	109.168(2)
V (Å ³)	542.37(12)	540.32(7)
Z	2	2
D_{calc} (g cm ⁻³)	3.577	3.574
T (K)	298(3)	298(3)
μ (mm ⁻¹)	5.332	5.345
Data collection		
Diffractometer	Bruker AXS SMART-APEX	Bruker AXS SMART-APEX
Scan type	ω	ω
θ range (°)	2–37.83 (completeness 96.5%)	2–38.19 (completeness 95.7%)
Absorption correction	SADABS	SADABS
Index ranges	$-26 \leq h \leq 26, -6 \leq k \leq 6, -17 \leq l \leq 17$	$-26 \leq h \leq 26, -6 \leq k \leq 6, -17 \leq l \leq 17$
Reflns measured	12326 (5041 after merging identical reflns)	13376 (5255 after merging identical reflns)
R_{int}	0.0601 (1590 unique reflns)	0.0717 (1602 unique reflns)
Refinement type	F^2	F^2
R_1^a	0.0558 (1283 reflns with $I > 2\sigma_I$)	0.0748 (1333 reflns with $I > 2\sigma_I$)
R_{all}	0.0756	0.0947
wR_2	0.1162	0.1384
GOF ^b	1.050	1.190
Refined parameters	74	74
Weighting scheme	$w = 1/[\sigma^2(F_o^2) + 11.17P]$ where $P = (F_o^2 + 2F_c^2)/3$	$w = 1/[\sigma^2(F_o^2) + 0.34P + 11.91P^2]$ where $P = (F_o^2 + 2F_c^2)/3$
(shift/e.s.d.) _{max}	0.000	0.000
max, min $\Delta\rho$ (e × Å ⁻³)	1.76, -2.14	1.87, -3.08

^a $R_1 = \Sigma||F_o| - |F_c|| / \Sigma|F_o|$.

^b GOF = $S = [\Sigma[w(F_o^2 - F_c^2)^2] / (n - p)]^{0.5}$, where n is the number of reflections and p is the total number of parameters refined.

between quartz and the reacting mixture, that was fired at 575 °C for 24 h and then slowly cooled down to room temperature [25]. Seemingly, the source of potassium could be tellurium tetrachloride used as transport agent, which was indeed found contaminated by K by EDS-EMPA analysis. This synthesis yielded crystals with $K_{0.23}(V_{5.35}Mo_{0.65})O_{15}$ composition. To further explore the compositional range of this material, a second synthesis has been carried out in the same conditions as described above but with a 1:2 $VO_2:MoO_3$ molar ratio. In this case crystals with the $K_{0.32}(V_{5.48}Mo_{0.52})O_{15}$ composition have been obtained. This quite surprising result can be explained by the fact that in this second case a larger amount of $VOMoO_4$ single crystals have been obtained.

Semi-quantitative EDS-EMPA analyses were also performed on the acicular single crystals obtained as described above by means of a Cambridge Stereoscan 200 scanning electron microscope equipped with a Link microprobe. The results were in good agreement with the formulae obtained by structure refinements.

2.2. X-ray single-crystal diffraction

Intensity data were obtained at room temperature on a Bruker AXS Smart Apex three-circle diffractometer equipped with a CCD detector using graphite monochromatized $MoK\alpha$ radiation ($\lambda = 0.71073 \text{ \AA}$). Data collections were carried out with operating conditions 50 kV and 30 mA. The Bruker SMART system of programs was used for preliminary crystal lattice determination and X-ray data collection. A total of 2240 frames (resolution: 512×512 pixels) were collected with four different goniometer settings ($\phi = 0^\circ, 90^\circ, 180^\circ, 270^\circ$) using the ω -scan mode (scan width: $0.3^\circ\omega$; exposure time: 50 s/frame; detector–sample distance: 4 cm). The Bruker program SAINT+ was used for the data reduction including intensity integration, background and Lorentz-polarization corrections. Final unit-cell parameters were obtained by the Bruker GLOBAL least-squares orientation matrix refinement procedure based on the positions of all measured reflections and are reported in Table 1. The

Table 2a

Fractional atomic coordinates, isotropic displacement parameters (\AA^2) and site occupancies for $K_{0.23}(V_{5.35}Mo_{0.65})O_{15}$

Atom	x/a	y/b	z/c	B_{iso}	Occupancy
K1	−0.0011(10)	0	0.4170(20)	3.44(48)	0.117(4)
V1	0.3359(1)	0	0.1036(1)	0.53(2)	1.0
V2	0.1162(1)	0	0.1181(1)	0.85(2)	0.673(3) V 0.327(3) Mo
V3	0.2887(1)	0	0.4141(4)	0.85(2)	1.0
O1	0	0	0	1.13(12)	1.0
O2	0.8148(2)	0	0.0512(4)	0.91(8)	1.0
O3	0.6338(2)	0	0.0775(4)	0.89(8)	1.0
O4	0.4355(3)	0	0.2157(4)	1.59(11)	1.0
O5	0.2634(2)	0	0.2243(4)	0.77(8)	1.0
O6	0.1059(3)	0	0.2744(4)	1.40(9)	1.0
O7	0.7556(3)	0	0.4234(4)	1.12(9)	1.0
O8	0.3972(3)	0	0.4711(5)	2.17(12)	1.0

Table 2b

Fractional atomic coordinates, isotropic displacement parameters (\AA^2) and site occupancies for $K_{0.32}(V_{5.48}Mo_{0.52})O_{15}$

Atom	x/a	y/b	z/c	B_{iso}	Occupancy
K1	0.0003(8)	0	0.4080(15)	2.47(34)	0.160(5)
V1	0.3371(1)	0	0.1054(1)	0.30(2)	1.0
V2	0.1168(1)	0	0.1184(1)	0.71(2)	0.742(4) V 0.258(4) Mo
V3	0.2888(1)	0	0.4147(4)	0.77(2)	1.0
O1	0	0	0	1.12(15)	1.0
O2	0.8157(3)	0	0.0543(5)	0.86(10)	1.0
O3	0.6337(3)	0	0.0761(5)	0.72(10)	1.0
O4	0.4364(4)	0	0.2185(6)	1.69(14)	1.0
O5	0.2639(3)	0	0.2242(5)	0.77(10)	1.0
O6	0.1077(4)	0	0.2735(5)	1.32(11)	1.0
O7	0.7554(4)	0	0.4230(5)	1.01(12)	1.0
O8	0.3974(4)	0	0.4734(6)	1.82(14)	1.0

Note: Standard deviations are in parentheses.

semi-empirical absorption correction of Blessing [26], based on the determination of transmission factors for equivalent reflections, was applied using the Bruker program SADABS [27]. The values of equivalent reflections were averaged and the resulting discrepancy factors are reported in Table 1. Structure refinements were carried out in space group $C2/m$ by full-matrix least squares using SHELXL-97 [28]. Atomic fractional coordinates of a natural bannermanite [20] were used as starting model. The atomic scattering curves were taken from the *International Tables for X-ray Crystallography* [29]. Structure factors were weighted according to $w = 1[\sigma^2(F_o^2) + (AP)^2 + BP]$, where $P = (F_o^2 + 2F_c^2)/3$, and A and B were chosen to produce a flat analysis of variance in terms of F_c^2 as suggested by the program. An extinction parameter x was refined to correct the structure factors according to the equation: $F_o = F_c k [1 + 0.001x F_c^2 \lambda^3 / \sin 2\theta]^{-1/4}$ (where k is the overall scale factor). All parameters, including anisotropic displacement parameters, site occupancies of cation sites and an isotropic extinction parameter, were refined simultaneously. No correlation greater than 0.61 and 0.57 for the two crystals, respectively, was observed. Final discrepancy factors, together with the goodness of fit S and the number of total and unique reflections, are reported in Table 1. We preferred to use the complete data sets collected up to $\sim 38^\circ\theta$ for the structure refinements in order to gain as much resolution to the structural model as possible, in particular for what concern cationic site populations. The apparently high R factors arise from this choice. With data sets filtered to $30^\circ\theta$, structure refinements converge to final R of 4.33% and 5.32% for the two crystals, respectively, within the average R -values reported in literature for similar phases. Atomic fractional coordinates, isotropic displacement parameters and site occupancies are reported in Tables 2(a) and (b). Bond distances and other geometrical parameters are given in Table 3.

3. Results and discussion

The crystal structure of $\beta\text{-K}_x(\text{V}_{6-y}\text{Mo}_y)\text{O}_{15}$ is depicted in Fig. 1. This compound crystallizes with the bannermanite-type structure in which all atoms are located in the special $4i$ position except for O1, which is located at the origin ($2a$ position). All atoms are then constrained to lie on plans at $y/c = 0$ or $y/c = \frac{1}{2}$. This is a common feature to other oxyvanadates and is a consequence of the short b dimension (~ 3.65 Å). General description of the bannermanite-type structure has been given by several authors [1,8,20,24].

Vanadium atoms are distributed on three different sites, which are drawn in Fig. 2. Substitution of vanadium with Mo^{6+} occurs only in the V2 position, as revealed by site occupancies refinement. This is in agreement with Galy et al. [30] who observed that molybdenum enters only the V2 position until its content equals half occupancy of the site (i.e., $y = 1$). V1 and V2 form distorted octahedra, as indicated by the rather high values of the distortion

Table 3
Bond distances (Å) and selected geometrical parameters

	$\text{K}_{0.23}(\text{V}_{5.35}\text{Mo}_{0.65})\text{O}_{15}$	$\text{K}_{0.32}(\text{V}_{5.48}\text{Mo}_{0.52})\text{O}_{15}$
<i>Site V1</i>		
V1–O4	1.594(4)	1.586(5)
V1–O2 $\times 2$	1.901(1)	1.896(1)
V1–O5	1.904(3)	1.904(5)
V1–O3	2.037(4)	2.034(5)
V1–O2	2.356(4)	2.384(5)
Mean of 6	1.949	1.950
Average edge length	2.715	2.716
OAV ($^\circ$)	136.03	135.41
OQE	1.054	1.055
V1–centroid	0.409	0.416
<i>Site V2</i>		
V2–O6	1.645(4)	1.625(5)
V2–O1	1.812(1)	1.810(1)
V2–O3 $\times 2$	1.910(1)	1.912(1)
V2–O5	2.182(4)	2.171(5)
V2–O2	2.292(4)	2.314(5)
Mean of 6	1.959	1.958
Average edge length	2.727	2.725
OAV ($^\circ$)	154.88	157.03
OQE	1.059	1.061
V2–centroid	0.415	0.420
<i>Site V3</i>		
V3–O4	1.588(5)	1.586(6)
V3–O5	1.840(4)	1.842(5)
V3–O7 $\times 2$	1.907(1)	1.906(2)
V3–O7	1.976(4)	1.978(5)
Mean of 5	1.844	1.844
Average edge length	2.798	2.884
<i>Site K1</i>		
K1–O8 $\times 2$	2.457(11)	2.458(10)
K1–O6	2.517(19)	2.464(16)
K1–O8 $\times 2$	2.580(12)	2.598(12)
K1–O4 $\times 2$	2.680(15)	2.650(12)
Mean of 7	2.564	2.554
Average edge length	3.235	3.226

Note: Standard deviations are in parentheses.

Site V2 is partially occupied by Mo (see text).

parameters octahedral quadratic elongation (OQE) and octahedral angle variance (OAV) [31] reported in Table 3. As is evident from Fig. 2(a), distortion of V1 octahedron is essentially due to the out-of-plane position of the central atom which lies 0.363 Å [in $\text{K}_{0.23}(\text{V}_{5.35}\text{Mo}_{0.65})\text{O}_{15}$; 0.489 Å in $\text{K}_{0.32}(\text{V}_{5.48}\text{Mo}_{0.52})\text{O}_{15}$] above the $\text{O2}^{\text{ii}}\text{–O2}^{\text{iii}}\text{–O3}^{\text{iii}}\text{–O5}$ equatorial plane; on the other hand the $\text{O4–V1–O2}^{\text{i}}$ angle is 176.7° [in $\text{K}_{0.23}(\text{V}_{5.35}\text{Mo}_{0.65})\text{O}_{15}$; 176.8° in $\text{K}_{0.32}(\text{V}_{5.48}\text{Mo}_{0.52})\text{O}_{15}$], indicating that the cation is nearly co-axial with the apical oxygen atoms. In the V2 polyhedron instead, the central atom lies only 0.185 Å [in $\text{K}_{0.23}(\text{V}_{5.35}\text{Mo}_{0.65})\text{O}_{15}$; 0.134 Å in $\text{K}_{0.32}(\text{V}_{5.48}\text{Mo}_{0.52})\text{O}_{15}$] above the $\text{O1–O3}^{\text{ii}}\text{–O3}^{\text{iii}}\text{–O5}$ equatorial plane but it occupies a more peripheral position within the octahedron. The $\text{O2}^{\text{i}}\text{–V2–O6}$ angle is in fact 159.1° [in $\text{K}_{0.23}(\text{V}_{5.35}\text{Mo}_{0.65})\text{O}_{15}$; 159.5° in $\text{K}_{0.32}(\text{V}_{5.48}\text{Mo}_{0.52})\text{O}_{15}$], as shown in Fig. 2(b). Such out-of-center displacement of

Mo^{6+} towards the most underbonded oxygen atoms in the polyhedron (O1 and O6, see Fig. 2b) helps reducing the Coulomb repulsion between cations occupying edge-sharing octahedra. V3 is in a square-based pyramid, as shown in Fig. 2(c), with O6 at 2.725 Å [in $\text{K}_{0.23}(\text{V}_{5.35}\text{Mo}_{0.65})\text{O}_{15}$; 2.693 Å in $\text{K}_{0.32}(\text{V}_{5.48}\text{Mo}_{0.52})\text{O}_{15}$] and hence not considered to be involved in the coordination polyhedron.

The valence bond (VB) approach [33] was applied to the two analysed crystals in order to find how differently charged vanadium ions are distributed among the sites. Site occupancies from structure refinements and the conventional r_0 -values of 1.803 for V^{5+} and 1.907 for Mo^{6+} were used for the calculations. In $\text{K}_{0.23}(\text{V}_{5.35}\text{Mo}_{0.65})\text{O}_{15}$, electroneutrality of the formula implies the presence of 0.88 V^{4+} ions (from K^+ and Mo^{6+} ions) out of 5.35 total vanadium atoms and hence an average positive charge of the vanadium atoms of 4.83. The valences at the three V positions were estimated as follows: V1 = 4.812; V2 = 5.097 (expected on the basis of site occupancies considering all vanadium atoms as pentavalent: 5.327); V3 = 4.829. Similarly, in $\text{K}_{0.32}(\text{V}_{5.48}\text{Mo}_{0.52})\text{O}_{15}$ electroneutrality requires 0.84 V^{4+} ions out of 5.48 total vanadium

atoms and hence an average positive charge of the vanadium atoms of 4.85. The valences at the three V positions were estimated as follows: V1 = 4.857; V2 = 5.083 (expected on the basis of site occupancies considering all vanadium atoms as pentavalent: 5.260); V3 = 4.836. Therefore, it seems that in both crystals there is no preferential site for V^{4+} . It is indeed difficult to locate the preferential site for V^{4+} since local charge balance and hence differently charged sublattices should be considered, as discussed by Galy et al. [30]. At any rate, from the VB analysis it follows that the lowest vanadium valence is estimated for the V2 ion, which appears to be slightly more charged than the others in agreement with the observations of Ozerov et al. [34], based on the results of multipole refinement, and Yamaura et al. [35].

On the light of the VB results, analysis of bond distances reveals that only the V1 and V3 polyhedra show the characteristic V = O vanadyl group (~ 1.59 Å), allowing to assume that these polyhedra might welcome V^{4+} . The shortest bond distance in the V2 polyhedron is 1.645 Å in $\text{K}_{0.23}(\text{V}_{5.35}\text{Mo}_{0.65})\text{O}_{15}$ and 1.625 Å in $\text{K}_{0.32}(\text{V}_{5.48}\text{Mo}_{0.52})\text{O}_{15}$. It is worth noting that the largest peak in the final difference-Fourier map in $\text{K}_{0.23}(\text{V}_{5.35}\text{Mo}_{0.65})\text{O}_{15}$ lies 0.55 Å from the V2 position and 1.590 Å from O6 indicating possible split positions for vanadium and molybdenum ions in this site which, unfortunately, could not be refined. Similarly for $\text{K}_{0.32}(\text{V}_{5.48}\text{Mo}_{0.52})\text{O}_{15}$. The apparent weakening of the double bond character in site V2 might be due to the presence of Mo^{6+} , which has a larger ionic radius (0.59 Å) [32] than V^{5+} (0.54 Å).

All the V–O bonds pointing toward the tunnel possess the double bond character (including V2–O6). The potassium atoms in the tunnels occupy the alternate positions named M1–M1' [11,30] and are coordinated by seven oxygen atoms with distances ranging between 2.457 and 2.680 Å (see Table 3).

Finally, the present work shows that the β -vanadium mixed bronzes structure can accommodate an extended range of alkali metal composition. In fact both $\text{K}_{0.23}(\text{V}_{5.35}\text{Mo}_{0.65})\text{O}_{15}$ and $\text{K}_{0.32}(\text{V}_{5.48}\text{Mo}_{0.52})\text{O}_{15}$ assume the β - $\text{Na}_x\text{V}_6\text{O}_{15}$ (bannermanite-type) structure, in which

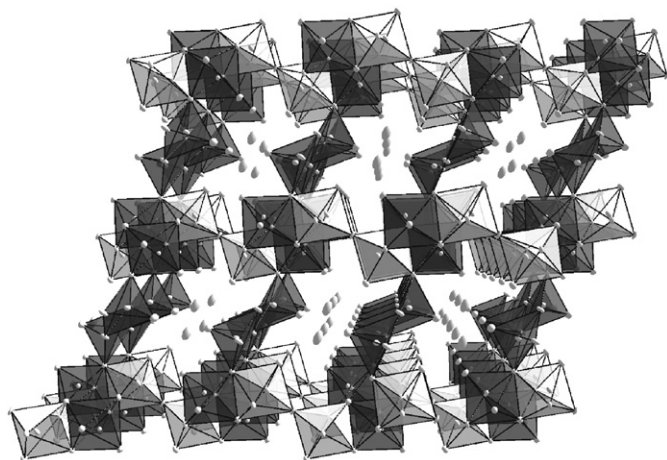


Fig. 1. Perspective view of the crystal structure of $\text{K}_x(\text{V}_{6-y}\text{Mo}_y)\text{O}_{15}$ along [010]. V1: dark octahedra; V2: light grey octahedra; V3: square-based pyramid.

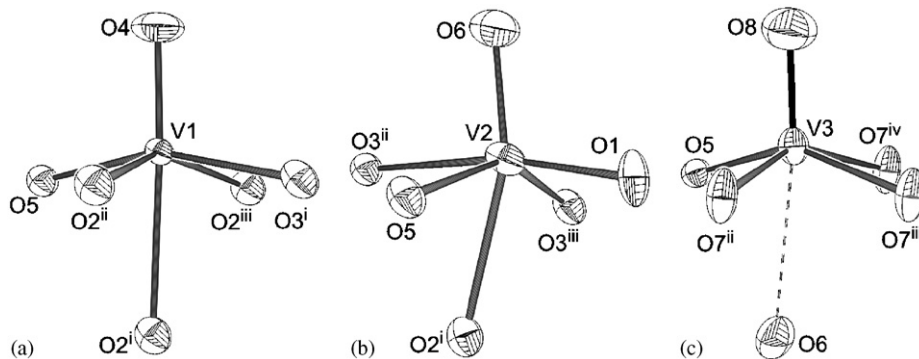


Fig. 2. Coordination polyhedra of vanadium ions: (a) site V1; (b) site V2; (c) site V3. Partial V–Mo substitution occurs in the V2 site. Thermal ellipsoids are drawn at the 80% probability level. Structural data of $\text{K}_{0.23}(\text{V}_{5.35}\text{Mo}_{0.65})\text{O}_{15}$ have been used. Symmetry codes: (i) $-x+1, -y, -z$; (ii) $x+\frac{1}{2}, y+\frac{1}{2}, z$; (iii) $x+\frac{1}{2}, y-\frac{1}{2}, z$; (iv) $-x+1, -y, -z+1$.

Mo substitutes for V only in the V2 position. This might be due to the distortion introduced by the molybdenum and further confirms the inherent structural flexibility of the coupled intercalant/framework system in this bronze family.

Further details of the crystal structure investigations can be obtained from the Fachinformationszentrum Karlsruhe, 76344 Eggenstein-Leopoldshafen, Germany (fax: +49 7247 808 666; e-mail: crysdata@fiz.karlsruhe.de) on quoting the depository numbers CSD 416778 for $K_{0.23}(V_{5.35}Mo_{0.65})O_{15}$ and 417164 for $K_{0.32}(V_{5.48}Mo_{0.52})O_{15}$.

References

- [1] R.L. Withers, P. Millet, Y. Tabira, Z. Kristallogr. 215 (2000) 357–363.
- [2] A. Hardy, J. Galy, A. Casalot, M. Pouchard, Bull. Chim. Soc. Fr. 4 (1965) 1056–1061.
- [3] J. Galy, J. Darriet, P. Hagenmuller, Rev. Chim. Miner. 8 (1971) 509–522.
- [4] D.W. Murphy, P.A. Christian, F.J. Di Salvo, J.V. Waszczak, Inorg. Chem. 18 (1979) 2800–2803.
- [5] J. Galy, J. Solid State Chem. 100 (1992) 229–245.
- [6] L. Permér, G. Ferey, Z. Kristallogr. 209 (1994) 413–417.
- [7] H.G. von Schnering, Yu. Grin, M. Kaupp, M. Somer, R.K. Kremer, O. Jepsen, T. Chatterji, M. Weiden, Z. Kristallogr. 213 (1998) 246.
- [8] V.A. Streltsov, P.N.H. Nakashima, A.N. Sobolev, R.P. Ozerov, Acta Crystallogr. B 61 (2005) 17–24.
- [9] R.P. Ozerov, Krystallografiya 2 (1957) 226–232 (in Russian).
- [10] H. Flood, H. Sorum, Tidsskrift Kjemi 5 (1943) 55.
- [11] A.D. Wadsley, Acta Crystallogr. 8 (1955) 695–701.
- [12] M. Pouchard, A. Casalot, J. Galy, P. Hagenmuller, Bull. Chim. Soc. Fr. 11 (1967) 4343–4348.
- [13] J.M. Savariault, J.L. Parize, D. Ballivet-Tkatchenko, J. Galy, J. Solid State Chem. 122 (1996) 1–6.
- [14] P. Millet, J.-Y. Henry, J. Galy, Acta Crystallogr. C 55 (1999) 276–279.
- [15] P. Hagenmuller, in: A.F. Trotman-Dickenson (Ed.), Comprehensive Inorganic Chemistry, vol. 4, Pergamon Press, New York, 1973, pp. 541–605.
- [16] T. Yamauchi, Y. Ueda, N. Mōri, Phys. Rev. Lett. 89 (2002) 057002–057004.
- [17] L.W. Shacklette, T.R. Low, L. Townsend, J. Electrochem. Soc. 135 (1988) 2669–2674.
- [18] O.A. Smirnova, A.M. Michailova, Yu.V. Seryanov, Russian J. Electrochem. 39 (2003) 1173–1177.
- [19] R.E. Stoiber, W.I. Rose, I.M. Lange, R.W. Birnie, Geologische Jahrb. 13 (1975) 193–205.
- [20] J.M. Hughes, L. Finger, Am. Miner. 68 (1983) 634–641.
- [21] L. Kihlborg, Acta Chem. Scand. 21 (1967) 2495.
- [22] P. Millet, C. Gasquères, J. Galy, J. Solid State Chem. 163 (2002) 210–217.
- [23] J. Darriet, J. Galy, P. Hagenmuller, J. Solid State Chem. 3 (1971) 596–603.
- [24] J. Darriet, J. Galy, P. Hagenmuller, J. Solid State Chem. 3 (1971) 604–613.
- [25] P. Carretta, N. Papinutto, C.B. Azzoni, M.C. Mozzati, E. Patarini, S. Gonthier, P. Millet, Phys. Rev. B 66 (2002) 1–11.
- [26] R.H. Blessing, Acta Crystallogr. A 51 (1995) 33–38.
- [27] G.M. Sheldrick, SADABS, Institut für Anorganische Chemie der Universität, Göttingen, Germany, 1996.
- [28] G.M. Sheldrick, SHELX97—Programs for Crystal Structure Analysis (Release 97-2), Institut für Anorganische Chemie der Universität, Göttingen, Germany, 1998.
- [29] J.A. Ibers, W.C. Hamilton, International Tables for X-ray Crystallography, vol. 4, Kynoch Press, Birmingham, UK, 1974, pp. 99–101.
- [30] J. Galy, J. Darriet, P. Casalot, J.B. Goodenough, J. Solid State Chem. 1 (1970) 339–348.
- [31] K. Robinson, G.V. Gibbs, P.H. Ribbe, Science 172 (1971) 567–570.
- [32] R.D. Shannon, Acta Crystallogr. A 32 (1976) 751–767.
- [33] I.D. Brown, D. Altermatt, Acta Crystallogr. B 41 (1985) 244–247.
- [34] R.P. Ozerov, V.A. Streltsov, A.N. Sobolev, B.N. Figgis, V.L. Volkov, Acta Crystallogr. B 57 (2001) 244–250.
- [35] J.-I. Yamaura, M. Isobe, H. Yamada, T. Yamauchi, Y. Ueda, J. Phys. Chem. Solids 63 (2002) 957–960.